Optics Communications 391 (2017) 135–140

Contents lists available at ScienceDirect

Optics Communications

journal homepage: www.elsevier.com/locate/optcom

A terahertz EO detector with large dynamical range, high modulation depth and signal-noise ratio

Xinjian Pan[a,b], Yi Cai[a,*], Xuanke Zeng[a,b], Shuiqin Zheng[a,b], Jingzhen Li[a], Shixiang Xu[a,*]

[a] Shenzhen Key Lab of Micro-Nano Photonic Information Technology, College of Electronic Science and Technology, Shenzhen University, Shenzhen, Guangdong 518060, PR China

[b] SZU-NUS Collaborative Innovation Center for Optoelectronic Science & Technology, Key Laboratory of Optoelectronic Devices and Systems of Ministry of Education and Guangdong Province, Shenzhen University, Guangdong 518060, PR China

ARTICLE INFO

Keywords:
Ultrafast optics
Electro-optical devices
Spectroscopy
Terahertz
Polarization-selective devices

ABSTRACT

The paper presents a novel design for terahertz (THz) free-space time domain electro-optic (EO) detection where the static birefringent phases of the two balanced arms are set close to zero but opposite to each other. Our theoretical and numerical analyses show this design has much stronger ability to cancel the optical background noise than both THz ellipsometer and traditional crossed polarizer geometry (CPG). Its optical modulation depth is about twice as high as that of traditional CPG, but about ten times as high as that of THz ellipsometer. As for the dynamical range, our improved design is comparable to the THz ellipsometer but obviously larger than the traditional CPG. Some experiments for comparing our improved CPG with traditional CPG agree well with the corresponding theoretical predictions. Our experiments also show that the splitting ratio of the used non-polarization beam splitter is critical for the performance of our design.

1. Introduction

In the past two decades, far infrared or terahertz (THz) region has been attracted great attention due to its unique optical properties. So far, THz technology based on ultrafast optics has been proven to be a very powerful tool and can be widely applied in many fields, e.g., THz spectroscopy, material dynamics, biomedical imaging, THz nonlinear optics, and so on [1–8]. There are two main techniques for free-space time domain THz field coherent detection, i.e. electro-optic (EO) sampling [9–15] and photoconductive antenna (PCA) [16–18]. PCA has stronger electric signal for collecting, while EO detection has higher bandwidth (> 10 THz) than PCA (< 3 THz) which is limited by the lifetime of the carriers in the photoconductor [18]. Generally, signal-to-noise ratio (SNR) of PCA for measurement of low frequency THz is lower than that of EO detection without lock-in amplification, but they are at the same level with lock-in amplification. More importantly, EO detection requires much lower probe power of laser and has greater performance and more convenient in parallel detections, e.g. THz imaging [19–21], single-shot THz detection by wavelength-encoding/space-encoding [22,23], etc.

For THz EO detection, special attention shall be paid to its optical modulation depth (OMD), linear dynamical range (LDR), and SNR besides its bandwidth. Until now, the EO sampling detection has been designed at the optical bias of either 45° [13] or near 0° [14]. Each of them has its own advantages and disadvantages. In comparison, the former, called THz ellipsometer, has larger LDR, but its poorer OMD means larger probe intensity is required, which can result in larger thermal noise and susceptible saturation for parallel detectors (e.g. CCD cameras). The latter, or crossed polarizer geometry (CPG), has much higher OMD, thereby needs much lower probe intensity, so is more suitable to be recorded by CCD. Unfortunately, its small LDR limits its applications. What is more, though the CPG can make this design operate at near zero optical bias point to reduce the background light [14], if balanced detection is used, its asymmetrical geometry can impair its ability to cancel the background noises [15].

It is desirable to develop a design that can combine their advantages. For this purpose, we had descripted and verified experimentally the THz EO detection with an improved theoretical model which considers the nonzero minimal transmission of the used polarizers and the polarization purity of probe laser [15]. Basing on this model, here we develop a novel design of THz EO detection with crossed polarizer geometry. Besides high OMD, this design exhibits simultaneously large LDR and excellent ability to cancel optical background noises [24], so we call it improved CPG. We believe that this work is very helpful to improve the applications of the THz detections, e.g. THz 2-D imaging [19–21] and material scattering detection [25].

* Corresponding authors.
E-mail addresses: caiyi@szu.edu.cn (Y. Cai), shxxu@szu.edu.cn (S. Xu).

http://dx.doi.org/10.1016/j.optcom.2017.01.021
Received 23 September 2016; Received in revised form 9 January 2017; Accepted 12 January 2017
Available online 23 January 2017

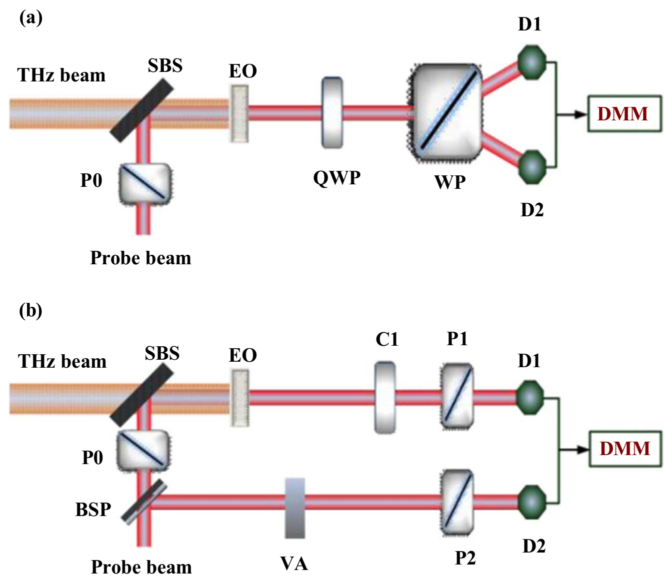

Fig. 1. Setups of the two **THz** EO detectors: **THz** ellipsometer [13] (a) and traditional CPG [14] (b). SBS: silicon beam splitter plate; M: mirrors; EO: EO crystal; BSP: beam splitter plate; QWP: quarter-wave plate; WP: Wollaston prism; VA: neutral filter; P0~2: linear polarizers; C1~2: birefringent phase compensators; D1~2: detectors; DMM: digital multi-meter.

2. The theoretical analyses

In order for the convenience of comparison, we firstly use our improved theory, which was verified by our experiments [15], to characterize the two traditional designs as shown in Fig. 1(a) (THz ellipsometer) and Fig. 1(b) (traditional CPG). Here, in Fig. 1(a), we use a 1 mm-thick high-purity silicon wafer as the beam splitter (SBS), both of whose surfaces are fine polished. THz beam transmits through the SBS and then enters an EO crystal, 1 mm < 110 > ZnTe crystal. After reflected by the SBS, the probe beam overlaps spatially with the THz beam inside the EO crystal. For the THz ellipsometer, after passing through the EO crystal and quarter-wave plate (QWP), the P and S polarized components of the probe are split by a Wollaston prism (WP), and are finally received by two receivers D1 and D2 of a balanced detector which is connected electrically to a digital multimeter (DMM, Keithley 2400). While, for the traditional CPG design as shown in Fig. 1(b), after through the EO crystal, the probe passes a variable phase compensator C1, a linear polarizer P1 (crossed to P0), and finally enters into D1, one receiver of the balanced detector. Another beam splitter plate (BSP) is set before P0 to get a beam which hits to D2, the other receiver of the balanced detector after through a neutral filter VA and a linear polarizer P2.

Suppose the probe, the input laser field of the polarizer P_0, can be expressed as $\mathbf{E}_0$=[E_{x0}, E_{y0}], so the corresponding laser intensity can be written as I_0=$|E_{x0}|^2$+$|E_{y0}|^2$=I_{x0}+I_{y0}. According to our description in reference 15, for the scheme in Fig. 1(a), the received probe intensities by D1 and D2 can be written as

$$I_1 = \frac{P_x}{2}\left(I_{x0}\cos^2\frac{\delta}{2} + \chi I_{y0}\sin^2\frac{\delta}{2}\right) \tag{1a}$$

and

$$I_2 = \frac{P_x}{2}\left(I_{x0}\sin^2\frac{\delta}{2} + \chi I_{y0}\cos^2\frac{\delta}{2}\right). \tag{1b}$$

Here P_x and P_y are the maximal and minimal transmittances of the polarizers respectively, so the extinct ratio of the polarizers is χ=P_y/P_x. The parameter δ stands for the total birefringent phase of one of the sub-beams, including the static birefringence from EO crystal δ_{EO}, the quarter-wave plate δ_{C} and the dynamical phase δ_{T} induced by THz field, i.e. δ=δ_{EO}+δ_{T}+δ_{C}≡α+δ_{T}.

When the THz is applied, or δ_{T}≠0, the output signal ΔI from the balanced detector shall be

$$\Delta I = -(P_x I_{x0} - P_y I_{y0})\sin(\alpha + \delta_T/2)\sin(\delta_T/2). \tag{2}$$

Suppose that we align the setup for balanced detection with δ_{T} =0 at the moment t_0, we shall have

$$(I_1 - I_2)|_{t=t_0} = \left(\frac{P_x I_{x0}}{2}\cos^2\frac{\alpha}{2} + \frac{P_y I_{y0}}{2}\sin^2\frac{\alpha}{2} - \frac{P_x I_{x0}}{2}\sin^2\frac{\alpha}{2} - \frac{P_y I_{y0}}{2}\cos^2\frac{\alpha}{2}\right)\Bigg|_{t=t_0} = 0. \tag{3}$$

From Eq. (3) we can see that the balance detection of this design depends on the laser intensity (I_{x0} and I_{y0}), polarizer (P_x and P_y), and the static birefringence phases (α, or δ_{C} and δ_{EO}). However, if $\delta/2$=$\alpha/2$=π/4, I_1≡I_2 with δ_{T} =0. For the α=π/2, Eq. (2) becomes

$$\Delta I = -\frac{P_x I_{x0} - P_y I_{y0}}{2}\sin\delta_T. \tag{4}$$

According to the description in reference 14, we can define the OMD of the balanced detection as

$$V = \frac{\Delta I}{I_1|_{\delta_T\neq 0} + 1_1|_{\delta_T=0} + I_2|_{\delta_T\neq 0} + I_2|_{\delta_T=0}}. \tag{5}$$

Correspondingly, the OMD of THz ellipsometer can be expressed as

$$V = \frac{(P_x I_{x0} - P_y I_{y0})\sin\delta_T}{2(P_x I_{x0} + P_y I_{y0})} \approx \frac{\sin\delta_T}{2}. \tag{6}$$

Now we turn our attention to the traditional CPG as shown in Fig. 1(b). Similarly, the received probe intensities by D1 and D2 shall be

$$I_1 = P_x\eta\left(P_y\cos^2\frac{\delta}{2} + P_x\sin^2\frac{\delta}{2}\right)I_{x0} + P_y\eta\left(P_x\cos^2\frac{\delta}{2} + P_y\sin^2\frac{\delta}{2}\right)I_{y0}. \tag{7a}$$

and

$$I_2 = (1-\eta)\gamma(P_y I_{x0} + P_x I_{y0}). \tag{7b}$$

Here η is the transmittance of the BSP, δ=δ_{EO}+δ_{T}+δ_{C1}=α+δ_{T}, δ_{C1} is the static birefringent phase from the variable phase compensator, γ is the attenuation coefficient of variable attenuator.

For balanced detection, it shall be required that

$$(I_1 - I_2)|_{t=t_0} = \left[\eta P_x P_y I_0\cos^2\frac{\alpha}{2} + \eta(P_x{}^2 I_{x0} + P_y{}^2 I_{y0})\sin^2\frac{\alpha}{2} - (1-\eta)\gamma(P_x I_{x0} + P_y I_{y0})\right]\Big|_{t=t_0} = 0. \tag{8}$$

Usually, we realize Eq. (8) by adjusting variable attenuator γ. At the presence of THz field δ_{T}, the output signal from the balanced detector is

$$\Delta I = I_1 - I_2 = \eta(P_x{}^2 I_{x0} + P_y{}^2 I_{y0} - P_x P_y I_0)\sin(\alpha + \delta_T/2)\sin(\delta_T/2). \tag{9}$$

Correspondingly, the OMD can be expressed as

$$V = \frac{(P_x{}^2 I_{x0} - P_x P_y I_0)\sin(\alpha+\delta_T/2)\sin(\delta_T/2)}{(P_x{}^2 I_{x0} + P_x P_y I_0) - (P_x{}^2 I_{x0} - P_x P_y I_0)\cos(\alpha+\delta_T/2)\cos(\delta_T/2) + 2(1-\eta)\gamma I_0}, \approx \frac{\sin(\alpha+\delta_T/2)\sin(\delta_T/2)}{2[\kappa - \cos(\alpha+\delta_T/2)\cos(\delta_T/2)]} \tag{10}$$

with the parameter

$$\kappa = \frac{I_{x0}/I_0 + P_y/P_x}{I_{x0}/I_0 - P_y/P_x}. \tag{11}$$

From Eqs. (2) and (9), we can make a comparison of the LDRs between the two designs in Fig. 1. In order to satisfy ΔI∝δ_{T}, it shall be required that α > > δ_{T} and sin(δ_{T})≈δ_{T}. Obviously, in Eq. (2), α=π/2, so sin(δ_{T})≈δ_{T} becomes the only requirement for the linear-dependence of